The compaction of gels by cells: a case of collective mechanical activity†

Pablo Fernandez* and Andreas R. Bausch*

Received 19th December 2008, Accepted 21st January 2009
First published as an Advance Article on the web 2nd February 2009
DOI: 10.1039/b822897c

To understand mechanotransduction, purely mechanical phenomena resulting from the crosstalk between contractile cells and their elastic surroundings must be distinguished from adaptive responses to mechanical cues. Here, we revisit the compaction of freely suspended collagen gels by embedded cells, where a small volume fraction of cells (osteoblasts and fibroblasts) compacts the surrounding matrix by two orders of magnitude. Combining micropatterning with time-lapse strain mapping, we find gel compaction to be crucially determined by mechanical aspects of the surrounding matrix. First, it is a boundary effect: the compaction propagates from the edges of the matrix into the bulk. Second, the stress imposed by the cells irreversibly compacts the matrix and renders it anisotropic as a consequence of its nonlinear mechanics and the boundary conditions. Third, cell polarization and alignment follow in time and seem to be a consequence of gel compaction, at odds with current mechanosensing conceptions. Finally, our observation of a threshold cell density shows gel compaction to be a cooperative effect, revealing a mechanical interaction between cells through the matrix. The intricate interplay between cell contractility and surrounding matrix mechanics provides an important organizing principle with implications for many physiological processes such as tissue development.

Introduction

The last years have witnessed a breakthrough of mechanics into biology as an essential aspect of the interaction of eukaryotic cells with their environments. Classical examples, such as hearing, structural optimisation by bones[1] or gravity sensing, do not reflect the generality of mechanotransduction responses. Mechanical tension, readily generated in tissues by the contractile activity of adhering cells undergoing shape changes and locomotion,[2–4] is a key factor regulating cell differentiation,[5–7] cell migration,[8] morphogenesis,[9–12] tissue remodeling and pathogenesis.[13,14] This rapidly growing body of knowledge is conferring mechanics with the status of an organising principle connecting tissue architecture and functionality to single cell shape, polarisation and differentiation. In particular, mechanics may hold the key to embryonic morphogenesis,[9,11,12] where convective tissue movements[15] and tension-dependent collective cell movements[10] play a crucial role.

Mechanical input can be of ''active'' nature, where the deformation of the extracellular matrix imposes a strain on the cell. This is the case in tissues such as bone or lung as well as in rheological experiments on cells.[16,17] Alternatively, in a ''passive input'' scenario, cells respond to external stiffness, a discovery which required the development of soft substrates with well-defined elastic properties.[18–20] Since the external medium plays here only a passive role, the cell needs active contractility in order to probe its surroundings and perform mechanosensing.[21] Therefore the distinction between passive and active input may be biologically meaningless: a cell probing its surroundings will exert an active input onto itself. Now along with the ability of the extracellular matrix to transmit stresses there is the fact that cells modulate their mechanical state in response to mechanical input. Extracellular stiffness has been shown to determine cell contractility[22] and stiffness[23] as well as the strength of focal contacts.[20,24,25] Thus, mechanical activity can feed back onto itself, a concept with

Lehrstuhl für Zellbiophysik E27, Technische Universität München, James-Franck-Strasse 1, D-85748 Garching, Germany. E-mail: pfernand@ph.tum.de. E-mail: abausch@ph.tum.de
† Electronic supplementary information (ESI) available: Details and video movies for gel compaction experiments. See DOI: 10.1039/b822897c

Insight, innovation, integration

By mixing cells and extracellular matrix components, one can investigate how the interplay between them leads to a functional structure. Cells inside a collagen network spontaneously shrink it down to 1% of its original volume within a few days, in an astonishing process which provides the simplest *in vitro* model system for tissue development. We show how it arises *via* a subtle interplay between cell contractility and biopolymer mechanics. Unexpectedly, cell polarization follows in time the contraction, hinting at a mechanism where cell shape is mechanically determined by that of the surroundings—possibly defining organizing centres in morphogenesis. Our results indicate that with its complicated mechanical properties, there is much more life in the extracellular matrix than hitherto realized.

striking implications for cell self-polarization[26,27] and collective cell behaviour.[28,29] Indeed, mechanical interaction between cells has been recently observed in endothelial cell migration.[30] This intricate mechanical interplay between cell and extracellular matrix offers fascinating prospects for tissue science but also complicates the identification of the causal biophysical parameters. It does not come as a surprise that the nature of the tension sensor is vague; proposed candidates range from mechanosensitive channels to cytoskeletal elements or even the nucleus itself.[21,27,31] At present, one of the most challenging problems in understanding mechanotransduction is distinguishing between cytomechanical regulation and the purely mechanical responses arising from the crosstalk between cell contractility and matrix mechanics.

Further complicating matters, in their physiological context cells are surrounded by soft extracellular matrix, distributed in three-dimensional arrangements with a tissue-specific architecture.[32,33] In three dimensions, large shape changes such as those involved in cell division or crawling imply large deformations of the surrounding matrix. One can therefore expect the rich nonlinear mechanics of biopolymer gels[34–39] to give rise to phenomena crucially different from those observed on 2D substrates. When Bell *et al.*[2] first studied collagen gels with embedded fibroblasts, they found a strikingly robust phenomenon involving indeed huge strains: a compaction by two orders of magnitude within a few days. This is a non-equilibrium process driven by the contractile activity of the embedded cells, since Cytochalasin B abolishes it. Despite the decades elapsed since its discovery and its relevance for fundamental questions in cell biology as well as for bioengineering applications, the biophysical mechanism underlying such large rearrangements of the matrix remains obscure. The volume shrinks by two orders of magnitude, wherein the volume fraction occupied by the cells is at most about 1%. So-called tractional forces generated during cell migration are thought to be essential to achieve the necessary local remodelling;[40] however, we lack a physical picture of them. The crucial role played by cell density is also not understood. Bell *et al.*[2] remark that the compaction rate depends on cell density in a ''distinctly nonlinear'' fashion, and Tamariz and Grinnell observed a change from purely local to global compaction upon increasing cell density by one order of magnitude.[40] Similarly obscure is the mechanism of the ''contracture'' which develops in cell-populated gels, a slow shortening process dominated by matrix remodelling leading to irreversible development of tension in the extracellular matrix.[13] Comparing gels reorganized by cells with centrifuged cell-free gels, Guindry and Grinnell observed similar, irreversible remodelling and concluded that cell-independent, non-covalent chemical interactions stabilized contracted collagen gels.[41] Though this finding strongly indicates that the key to irreversible remodelling of connective tissue is mechanics rather than biochemistry, presently the discussion focuses on the importance of metalloproteinases.[13]

Here, we take a close look at the compaction of free collagen gels by embedded cells. Aiming at a quantitative analysis of the physical aspects, we finely control gel geometry and cell distribution and follow in time the strain field. For an extensively scrutinized phenomenon, collagen compaction provides remarkably novel insight into tissue mechanics. The shrinkage of the gel arises from cell contractility in an unexpected manner: *via* a cooperative effect taking place at the boundaries and propagating into the bulk. As a consequence of its nonlinear mechanical properties, the collagen gel compacts irreversibly and becomes anisotropic, in a purely mechanical contracture-like process. Our results can be understood in terms of an interplay of mechanical interaction between cells and the anisotropic mechanical response at the boundary. We further introduce the working hypothesis of active, but non-adaptive contractility as a crucial ingredient in mechanosensing, emphasizing the need of a global approach to cell and matrix.

Results

Cells are known to exert forces to their environment. Once MC3T3-E1 osteoblast cells are embedded in collagen gels, processes such as migration or cell division locally deform the surrounding network. Remarkably, global deformations are not observable in the bulk of the gel, but only close to its boundaries. This global effect is therefore best studied in thin collagen gels where the influence of the boundaries can be precisely determined. In order to simplify the analysis, we distribute cells evenly over the non-adhesive bottom of the pattern, thereby achieving a 2D distribution of cells embedded in a 3D matrix (see Fig. 1). By control experiments where cells are uniformly distributed throughout the bulk of the collagen it is ensured that qualitatively similar behaviour is observed. In rectangular gels with an aspect ratio of 20 and a mean separation between cells of about 50 μm a large, uniform contraction of the gel sets in immediately after gelation. Within a few hours, the initial cross-section δ_0 of a 250 μm wide gel reduces down to $\delta \sim 100$ μm (see Supplementary Movie 1, ESI†).

The contraction is highly anisotropic as visualized by tracing the displacement of embedded beads (as described in Materials and Methods). Comparing the axes parallel and perpendicular to the boundary of the gel shows that the contraction takes place mostly in the perpendicular direction (see Fig. 2). The perpendicular contraction $\lambda_\perp$ changes by about one order of magnitude more than the contraction parallel to the boundary $\lambda_\parallel$ (Fig. 2). In this process the total volume of the collagen gel decreases, as indicated by the detachment of the gel from the interface and the appearance of a pure solution phase (Fig. 1 and Supplementary Movie 1, ESI†). The anisotropic contraction is clearly a consequence of the presence of the boundaries: further away from the edge the contraction lags behind and is significantly slower (Fig. 3). At distances larger than 500 μm from the boundary no contraction is observable at all. These results can be well understood in terms of the mechanical anisotropy imposed by the gel boundaries. For any elastic material, the response to forces parallel to a free boundary is significantly stronger than the response to perpendicular forces.[29] As a consequence, isotropic forces close to the boundary will directly produce an anisotropic contraction perpendicular to the surface. This is consistent with the finding that most cells are still round

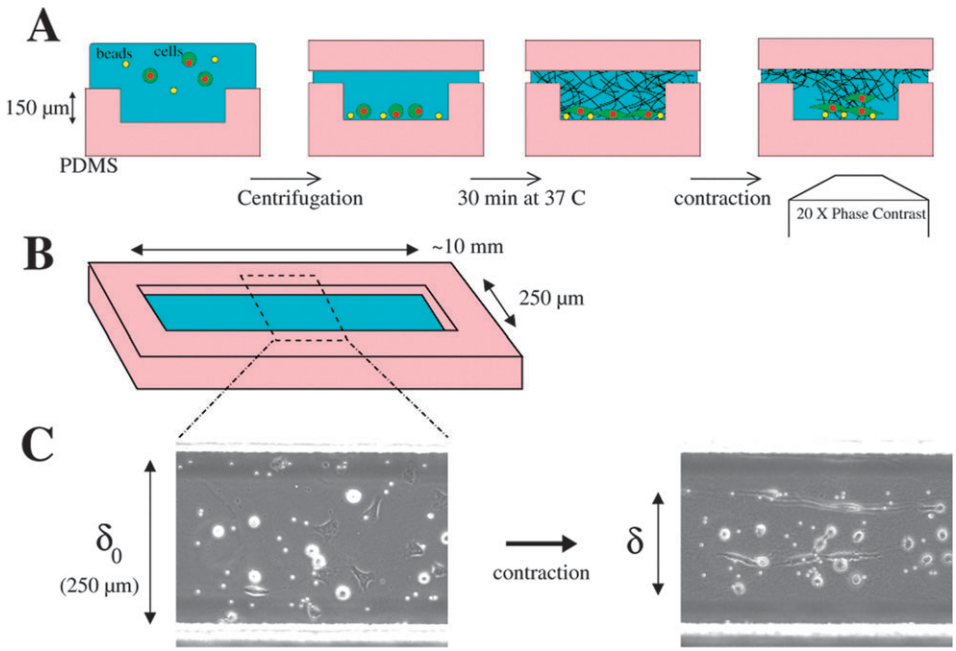

Fig. 1 Experimental procedure. (A) The suspension of cells and beads in neutral collagen solution is poured onto the hydrophobic PDMS pattern. Cells and beads are centrifuged down before gelation, in order to achieve a 2D distribution and thereby simplify the geometry. In about 30 min at 37 °C collagen gelates. From the phase contrast images one can follow the displacement of the embedded beads and infer the strain in the gel. (B) Only a section in the middle of the long rectangular gel is observed. (C) Within a few hours osteoblasts contract the gel by up to 50%. Notice that the short edges of the gel are outside the field of view and cannot be seen in these images. This contraction of a thick gel by a single layer of cells resembles the experiment by Grinnell and Lamke.[55]

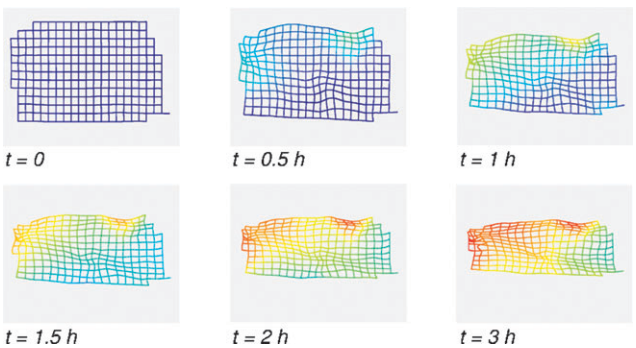

Fig. 2 Time series of the contraction of a 250 μm-wide collagen slab by MC3T3-E1 osteoblasts at a large cell density. The black grid, representing the initial state of the gel, is obtained by interpolating the initial positions of the beads. By distorting the initial grid with the strain field in the gel (calculated as described in Materials and Methods) we obtain the coloured grids. The colour code gives the perpendicular contraction $\lambda_{\perp}$. Notice that the grid does not represent the full gel, but only the middle section, as in Fig. 1. In particular, the short edges are not the boundaries of the gel.

during the initial contraction phase, where the deformation takes place at its fastest rate (Fig. 4). Significant cell elongation and alignment parallel to the boundaries of the gel, a phenomenon equivalent to that found in ref. 42, can only be seen after the contraction is completed. Therefore, the observed anisotropic gel contraction is prerequisite for cell alignment and cannot be understood as a consequence of cell alignment.

When the activity of myosin motors is inhibited by blebbistatin[43] (50 μM) from the beginning of the gelation, no contraction is observed at all. Addition of blebbistatin a few hours after gelation stops the ongoing contraction and a significant elastic recovery is observable (~5%) (Fig. 5). Irreversibly damaging CFSE-labeled osteoblasts by high power irradiation has the same effect. Thus the largest part of the contraction (35%) is a plastic deformation of the collagen gel resulting from active myosin contraction. In agreement, Guidry and Grinnell observed that the compaction of fibroblast-populated collagen gels persisted after removing cells by a treatment with detergent.[41]

If the contraction process is purely determined by the mechanical properties of the matrix, not only internal forces but also external forces should be sufficient to induce gel compaction. This is indeed the case, as can be seen by imposing external forces to pure collagen gels without embedded cells. By surrounding the collagen solution drop in a silicon oil phase, we prevent water evaporation and ensure constant volume of the collagen solution. After gelation takes place the collagen gel has initially the shape of the drop. Then, we stretch the drop by moving a slidable wall, imposing a stretch rate of 1% s^{-1} (Fig. 6). For small deformations the response is elastic dominated and fully reversible. Upon large deformation (about 40%) the gel shrinks significantly and a pure solution phase appears. About simultaneously, anisotropic arrangements of thick fibers become observable. This process is irreversible: once the external force is released the gel remains in the contracted state for weeks. Note that the deformation of the drop is always volume-preserving, since

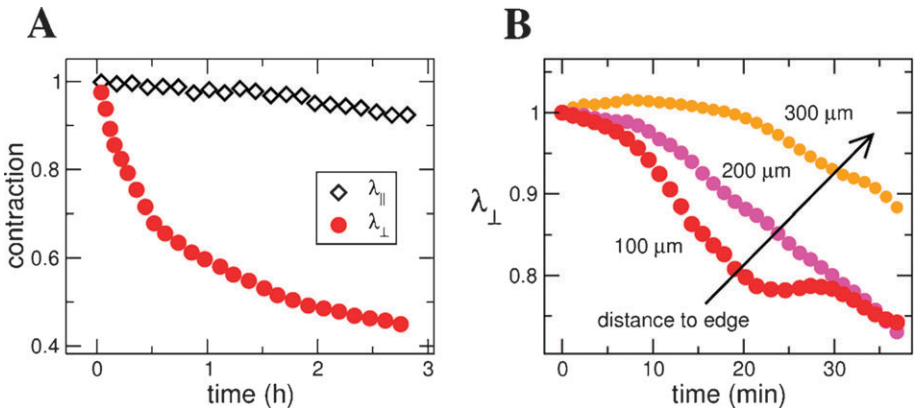

Fig. 3 (A) Contraction factors as a function of time, for the directions parallel $\lambda_{\parallel}$ and perpendicular $\lambda_{\perp}$ to the long axis. Gel width was 250 µm. (B) Contraction factor $\lambda_{\perp}$ (perpendicular to the gel axis) as a function of time, for different values of the distance to the gel boundary. Gel width was 1 mm. Experiments were performed with MC3T3-E1 osteoblasts.

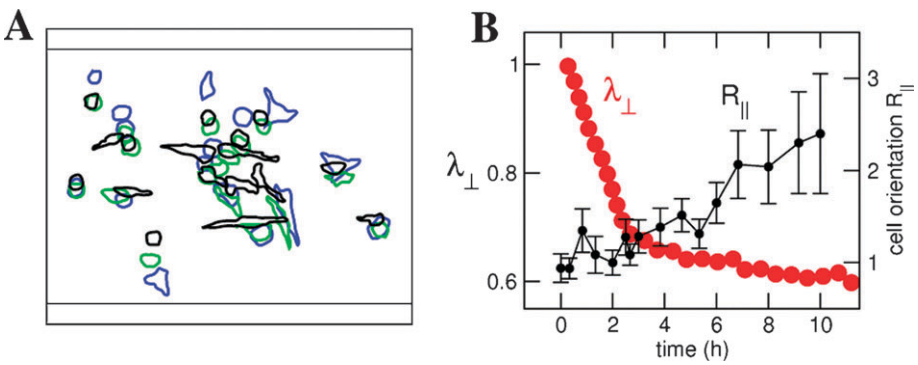

Fig. 4 Comparison of gel contraction and cell alignment shows that the former takes place before cells align. (A) cell contours during gel contraction, at times 20 min (blue), 3 h (green) and 8 h (black) after gelation. (B) Average cell orientation along the long axis $R_{\parallel}$ and perpendicular contraction $\lambda_{\perp}$ as a function of time. Cell orientation is defined in terms of the aspect ratio R and the cell angle α as $R_{\parallel} = R\cos(\alpha)$. Error bars are standard errors ($n = 18$ cells). Gel width was 250 µm. The experiment was performed on MC3T3-E1 osteoblasts.

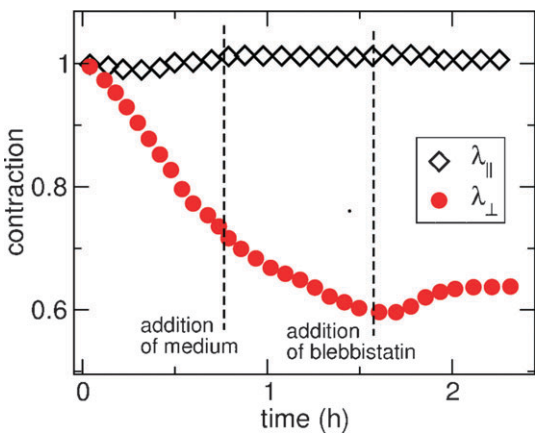

Fig. 5 Addition of Blebbistatin kills the ongoing contraction and relaxes the strain by about 5%. The remaining 35% is a plastic deformation. Medium without blebbistatin was first introduced as a negative control. Gel width was 250 µm. The experiment was performed on MC3T3-E1 osteoblasts.

water is essentially incompressible; the shrinkage of the gel inside the drop is therefore a nontrivial consequence of its nonlinear mechanical response.‡ We conclude that cells attain irreversible compaction by applying mechanical forces, without resorting to biochemical means.

If the observed phenomenon is defined by the gel response to force, then it should crucially depend on cell type, collagen stiffness, and cell density. Depending on the forces a certain cell type is able to exert, gel stiffness and cell density will determine whether a compaction is observed. Primary osteoblasts induce an anisotropic contraction process at the same cell density and collagen stiffness as observed for the MC3T3-E1 (see ESI and Supplementary Movie 2†). In contrast, 3T3 fibroblasts are unable to induce a significant large-scale contraction of the gel—even at very large density (see ESI and Supplementary Movie 3†). Fibroblasts migrate extensively through the gel and extend long protrusions, whereby inducing only small (less than 5%) local deformations. However, upon lowering the collagen concentration by a

‡ A similar deformation field, namely contraction along a single axis, can be achieved by means of confined compression, where a porous piston compacts the collagen gel while allowing the solution to flow out. With this approach, Chandran and Barocas also observed irreversible collapse of collagen gels.[39]

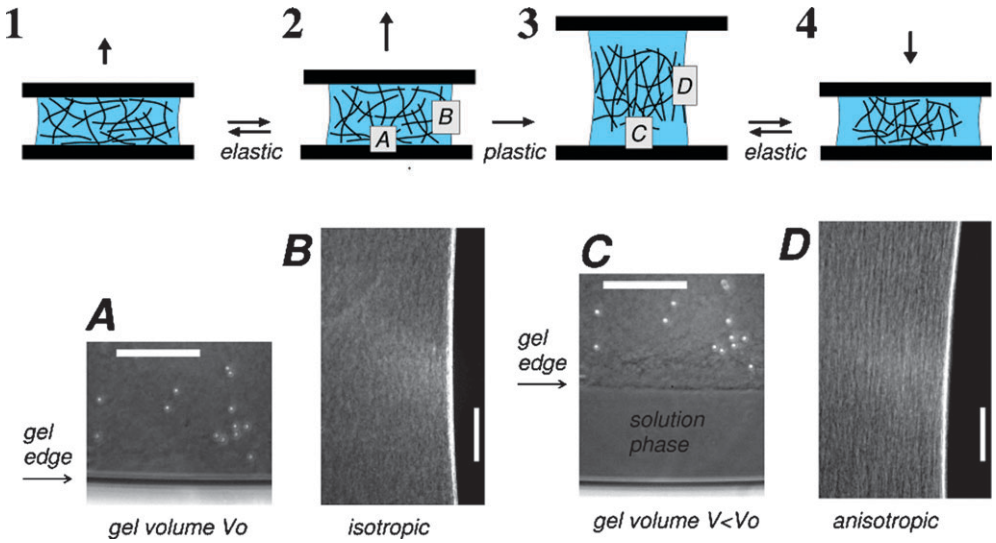

Fig. 6 Stretching a drop of collagen gel leads to irreversible compaction and fiber orientation. As the hydrogel is deformed beyond the linear regime (2 → 3), it compacts; at the free boundaries a pure water phase appears (A → C). Beads were added in order to reveal the translation of the gel. From the phase contrast images, fiber alignment along the main stretch direction can be observed (B → D). The deformation is plastic: as the drop is deformed back to the initial state, the process does not revert within the observation time of two weeks. The collagen gel has become irreversibly smaller and anisotropic. Bars: 100 μm.

factor of two and thereby decreasing the stiffness of the surrounding matrix from 14 to 2 Pa (as measured with a shear rheometer) a significant anisotropic compaction can be observed, quantitatively slower but qualitatively similar to the effects observed with osteoblasts (see ESI and Supplementary Movie 4†). This would indicate that the total forces exerted by the cells need to be sufficiently high to induce the effect. Thus lowering the cell density should suppress global deformations. Indeed, at low cell concentrations no significant deformation of the gel is observed. Cells migrate through the gel, without straining it locally by more than 5%. Only at higher densities the gel contraction appears: the initial gel contraction increases in a strongly nonlinear manner with osteoblast density, jumping from zero to a roughly constant value at a cell density of $\sim 10^{-4}$ μm^{-2} corresponding to a separation between cells of about 100 μm (Fig. 7). Observing heterogeneous osteoblast densities within gels supports the finding of a density threshold: whereas isolated cells migrate in a random manner, a higher density cluster of cells remains stationary and contracts the gel anisotropically (see Supplementary Movie 5, ESI†). The existence of a critical cell density shows that gel compaction takes place through a cooperative effect, implying mechanical interaction between cells.

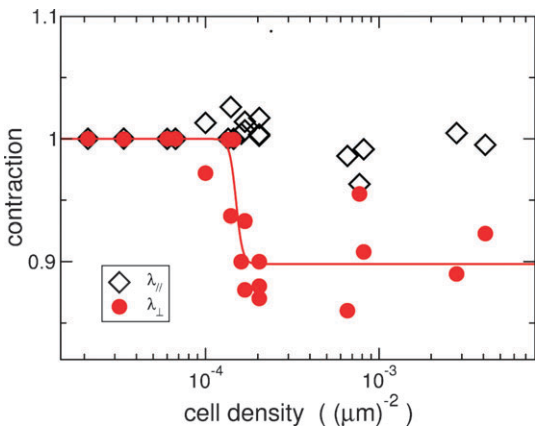

Fig. 7 Contraction as a function of two-dimensional cell density, for the direction perpendicular ($\lambda_\perp$) and parallel ($\lambda_\parallel$) to the long axis of the gel. The stretch factors were taken at 1000 s after the gelation, in order to minimize the influence of mechanical nonlinearities at larger deformations. Gel width was 250 μm. Experiments were performed on MC3T3-E1 osteoblasts.

Discussion

Taken together, the observed gel contraction and cell alignment processes are the result of the mechanical properties of the surrounding matrix. Cells seem to apply tension "blindly" to the gel, the anisotropic contraction following solely from the anisotropic response at the boundary. The cells as contractile elements need a critical density to be able to force the gel to contract at the boundary. Isolated cells do not notice the boundary, even though the anisotropical mechanical response could in principle be detected by an arbitrarily small deformation.[29] The critical density is not only set by the forces the individual cells are able to exert but, importantly, by the superposition of the complicated strain fields propagating within the network. The critical distance should thus be given by the penetration depth of the strain field, which for small deformations will be approximately the size of the cell. Accordingly, we observe a critical mean separation between cells of about 100 μm. The clear-cut jump in the cell density dependence puts on a firm footing previous observations suggesting a cooperative effect, such as the importance of cell density in cell-realignment mentioned by Takakuda and Miyairi[42] and the observation of Eastwood *et al.* that cells tend to align along chains.[44] Interestingly, recent observations of mechanical interaction between cells crawling on a 2D substrate showed an interaction length of the order of 30 μm.[30]

As the contraction progresses, remarkable mechanical phenomena show up which involve the rich nonlinear mechanics of biopolymer gels.[34–39] The large forces exerted by the cells irreversibly compact the matrix. Irreversibility has a far-reaching implication: the past strain history of the material is permanently stored into its microstructure. This observation sheds light on contracture phenomena, where the tension developed by cell contraction remains after cell death.[13] Crosslink formation or biochemical "shortening" have been invoked to explain this phenomenon; however, as shown here, contracture can be achieved in a purely mechanical fashion by means of externally applied forces. Analogous conclusions were found with a different approach by centrifuging collagen gels.[41] Incidentally, the fact that cells located at free boundaries can attain these large forces indicates the presence of three-dimensional internal stress fields. A common occurrence in many materials, among them biopolymer networks,[45] internal stresses invalidate the frequent assumption that free gels cannot develop significant tension.[13,14]

As a further consequence of the nonlinear mechanics of biopolymer gels, a large deformation will induce structural anisotropy by irreversibly aligning collagen fibers. This suggests a simple explanation for cell alignment parallel to the boundaries, in agreement with reasoning from ref. 3 and 42. After the large contraction, the anisotropic environment can provide a directional template for biochemical polarization and further cell elongation. Alignment can be thus be seen as slaved to gel contraction by the plastic deformation.

The intricate mechanical matrix response may be crucial to explain complex cell behaviors as found in embryogenesis or tissue development, where large deformations are involved and mechanical tension is known to be essential.[9–12,15] Alternatively, an active mechanosensing process has been postulated, where cells detect the stiffer spatial directions and exert forces preferentially along them, equivalent to minimizing the work invested in achieving a given tension.[26,29,46,47] This principle leads to cooperative effects: contractile activity along a particular direction renders the matrix stiffer, prompting neighbouring cells to further pull along it.[29,46] While such an active response seems not to be necessary to explain the described gel compaction and cell alignment effects, it may well be that it sensitively modulates cellular responses. Elaborate biomechanical and biochemical efforts are needed to identify which parts of the cell alignment process rely on such active sensing mechanisms.

The reasoning outlined above hints at a generic mechanism to translate the shape of a tissue into its biochemical structure. It has been realized before that tissue shape crucially influences the development of tension by contractile cells;[44] in turn, tension will modulate cell behaviour,[13] giving rise to spatial patterns of cell and matrix organization[48] as well as cell proliferation[49] as a function of predefined boundary conditions and tissue shape. The present mechanism extends the influence of tissue geometry to irreversible changes in matrix microstructure without the need for regulation of cellular activity. Therefore, this mechanism can be extrapolated to any isotropic distribution of contractile elements inside a biopolymer gel. Importantly, contractility need not be limited to classical molecular motors; crosslinker binding could similarly provide the driving force.[45] Such a purely mechanical structure-follows-shape principle may thus arise at disparate length scales from tissues down to the cytoskeleton.

Conclusions

In summary a new paradigm needs to be explored—with its complicated mechanical properties, the extracellular matrix has much more life in it than hitherto realized. Where extensive tissue deformations take place, neglecting the mechanical crosstalk between cell and matrix may be removing a crucial actor from the scene. As modern cell biology moves towards a holistic conception, we may have to accept that fate of cells arises as a compromise between their interests and those of the environment.

Materials and methods

Cell culture

MC3T3-E1 osteoblasts[50] and 3T3 fibroblasts[51,52] from the German Collection of Microorganisms and Cell Cultures[53] were cultured in DMEM medium (PAA, Austria) with 10% fetal bovine serum following standard procedures. Primary osteoblasts were a gift of Rainer Burgkart (Klinikum rechts der Isar, Technische Universität München). They were obtained from cancellous bone isolated during hip implantations as a cell-pool of six patients. Their use for scientific purposes was approved by the local Ethics Committee. Primary osteoblasts were cultured until passage eight at 37 °C and 5% CO_2 in alpha-medium with 3% FBS, 2% HEPES buffer, 0.2% Primocin, 1% MEM Vitamine, 1% L-glutamine, 0.5% ascorbic acid and 0.02% dexamethasone.

Collagen gel

Collagen gels were made from PureCol bovine collagen, about 97% Type I collagen at an approximate concentration of 3 g L^{-1} (Nutacon b.v., Leimuiden, Netherlands). To prepare 10 ml of neutral collagen solution for an experiment, first 1 ml of Dulbecco's modified Eagle medium 10× (PAA) and 0.3 ml of μl of 1 M HEPES buffer (PAA) were added to 7.85 ml of PureCol. The solution was then neutralized by addition of 0.25 ml of 1 M NaOH. Finally, 0.3 ml FBS and 0.3 ml of a penicillin–streptomycin mixture (PAA) were added. So-prepared solutions were kept at 4 °C for up to three weeks.

Experimental procedure

Prior to an experiment, non-confluent cells were starved for one night in order to synchronize them. First experiments conducted without previous starvation had shown similar results, indicating that location within the cell cycle is not relevant for the gel compaction process. After starvation, cells were trypsinized for 5 min and centrifuged for 5 min at 400 g. The pellet was washed with PBS and resuspended in the (neutralized) collagen solution. Collagen-coated 6 μm-diameter latex beads were added and this suspension was poured onto clean, dry PDMS patterns. Centrifuging the pattern at 1000 *g* for 4 min made cells and beads sink to the PDMS bottom and removed the bubbles trapped in the

(hydrophobic) patterns. Control measurements where cells were distributed throughout the gel were performed by slowly rotating the sample during gelation. Since these samples showed similar behaviour, we concentrated here on the 2D distributed cells, for the sake of simplicity and sound quantification. Cells are still embedded in a 3D matrix environment and it is ensured that the strain in only one plane can be accurately quantified by the embedded beads.

To provide mechanical stability and prevent the collagen gel from slipping out of the PDMS substrate, a $\sim$1 mm thin slab of PDMS was placed on top of the collagen solution. The pattern was finally placed on the microscope stage in a heating unit at 37 °C. Collagen gelation began in about 15 min and was complete within 30 min, as could be seen from the phase contrast images where the gel appears as a dense network of fibers. Neither the collagen gel nor the cells adhere significantly to the hydrophobic PDMS substrate; the procedure thus provides a reproducible no-adhesion condition at the boundary. In the absence of cells, the collagen gel fills the available volume and does not shrink significantly. In presence of cells at a large density, gel contraction takes place. Judging from the phase-contrast images, we do not observe signatures of collagen production or hydrolysis within the first 20 h. Non-synchronized cells are seen to divide inside the gel. Cell death is not observed within the first two days.

Blebbistatin was added to the medium and the medium was added to the sample through small holes in the covering PDMS. The solution was dragged into the matrix by gravity.

Gel deformation analysis

We measure the deformation of the collagen gel by tracking embedded collagen-coated beads. A main advantage of the experiment is that a two-dimensional analysis of the deformation suffices, since cells and beads lie evenly on the bottom of the pattern. As a control, experiments done varying the pattern depth between 50 and 200 μm gave qualitatively similar results. However, a local measure of strain is necessary due to the heterogeneity in cell distribution. From the position of three beads one can unequivocally define two material vectors $\boldsymbol{R}_1$, $\boldsymbol{R}_2$ (Fig. 8A). For a meaningful measure of the local strain, the beads must be close to each other and must not lie on the same line. The contraction of the gel by the cells moves these beads to new locations and the material vectors change to $\boldsymbol{r}_1$, $\boldsymbol{r}_2$ (Fig. 8A). From the initial and final vectors we define a deformation gradient matrix $\boldsymbol{\Lambda}$,

$$(\boldsymbol{r}_1, \boldsymbol{r}_2) = \boldsymbol{\Lambda}(\boldsymbol{R}_1, \boldsymbol{R}_2).$$

The deformation gradient conveys the local deformation of the gel. To distinguish between mechanically meaningful stretches and irrelevant rotations, a polar decomposition[54] is applied to the deformation gradient

$$\boldsymbol{\Lambda} = \boldsymbol{RS},$$

to split it into a symmetric part $\boldsymbol{S}$ corresponding to a pure distorsion and an orthogonal part $\boldsymbol{R}$ representing a rigid-body rotation. Finally, since the experiment is restricted to gels with rectangular shapes, the natural deformation measure is given by the stretch factors along the directions parallel $\lambda_{\|}$ and perpendicular $\lambda_{\perp}$ to the long axis,

$$\lambda_{\|} = \boldsymbol{r}_{\|} \cdot \boldsymbol{S}\, \boldsymbol{r}_{\|}$$

$$\lambda_{\perp} = \boldsymbol{r}_{\perp} \cdot \boldsymbol{S}\, \boldsymbol{r}_{\perp}$$

If the contraction is uniform, then the perpendicular stretch factor boils down to $\lambda_{\perp} = \delta/\delta_0$ (see Fig. 1). In the general case of a non-uniform deformation, the stretch factors provide a local measure. Knowing the constitutive relation of the material, one could in principle estimate the stress from the stretch matrix $\boldsymbol{S}$. This is in practice extremely difficult; since cells contract collagen by a large amount, nonlinear viscoelastic and plastic effects have to be taken into account. For the present work, it is safer and more honest to limit ourselves to the stretch factors.

Cell orientation analysis

Throughout the experiment, most cells are either round or have a well-defined axis. Cell elongation and alignment parallel to the long axis of the rectangular gel is immediately recognized with the naked eye. The question naturally arises whether this alignment is causally related to the contraction; it is therefore desirable to quantify its extent. For this, cells contours were manually traced and the geometrical centers of the cells calculated from them. The cell axis was defined by looking for the maximum contour distance from the cell center (Fig. 8B). In most cases this was a well-defined magnitude, and the distance between contours along the cell axis provided a measure of the cell length L. Taking the cell width W at the direction perpendicular to the cell axis (Fig. 8B) allowed defining a cell aspect ratio $R = L/W$. Finally, to quantify both elongation and alignment, we defined

$$R_{\|} = R\cos(\alpha),$$

where α is the angle between the cell axis and the direction parallel to the gel axis, $\boldsymbol{r}_{\|}$. This magnitude provides a meaningful measure of the anisotropy of the cell shape. When averaging over many cells as in Fig. 4, values $R_{\|} > 1$ imply both elongation and alignment parallel to the gel axis.

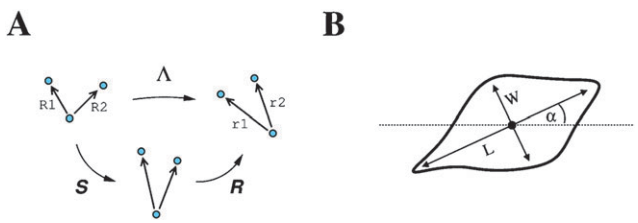

Fig. 8 (A) Measurement of the local strain from the displacement of embedded beads. By applying a polar decomposition to the deformation, the physically relevant true stretch $\boldsymbol{S}$ can be separated from the irrelevant rotation $\boldsymbol{R}$. (B) The cell center is defined as the center of mass of the cell contour. In turn, the maximum distance between contour and center of mass defines the cell axis. Dividing the cell length L by the width W perpendicular to the cell axis defines the aspect ratio $R = L/W$. A measure of orientation along the x-axis is given by $R_{\|} = R\cos(\alpha)$.

Acknowledgements

It is a pleasure to thank Ulrich Schwarz and Frederick Grinnell for their critical reading of the manuscript along with many helpful suggestions. We also gratefully thank Petra Kleiner and Rainer Burgkart (Klinikum rechts der Isar, Technische Universität München) for their generous gift of primary osteoblasts as well as inspiring discussions and advice, Markus Harasim and Bernhard Wunderlich for assistance with the PDMS substrates, Gabi Chmel and Monika Rusp for technical assistance, and Sebastian Rammensee for reading the manuscript. This work was supported by the Deutsche Forschungsgemeinschaft through the DFG Cluster of Excellence, the Nanosystem Initiative Munich (NIM) and the International Graduate School of Science and Engineering (IGSSE).

References

1 C. H. Turner, *Ann. N. Y. Acad. Sci.*, 2006, **1068**, 429.
2 E. Bell, B. Ivarsson and C. Merril, *Proc. Natl. Acad. Sci. U. S. A.*, 1979, **76**, 1274.
3 A. K. Harris, D. Stopak and P. Wild, *Nature*, 1981, **290**, 249.
4 L. K. Wrobel, T. R. Fray, J. E. Molloy, J. J. Adams, M. P. Armitage and J. C. Sparrow, *Cell Motil. Cytoskeleton*, 2002, **52**, 82.
5 G. H. Altman, R. L. Horan, I. Martin, J. Farhadi, P. R. H. Stark, J. C. R. Volloch and D. L. Kaplan, *FASEB J.*, 2001, **15**, 270.
6 B. T. Estes, J. M. Gimble and F. Guilak, *Curr. Top. Dev. Biol.*, 2004, **60**, 91.
7 A. J. Engler, S. Sen, H. Lee Sweeney and D. E. Discher, *Cell*, 2006, **126**, 677.
8 C.-M. Lo, H.-B. Wang, M. Dembo and Y. L. Wang, *Biophys. J.*, 2000, **79**, 144.
9 M. Krieg, Y. Arboleda-Estudillo, P.-H. Puech, J. Käfer, F. Graner, D. J. Müller and C.-P. Heisenberg, *Nat. Cell Biol.*, 2007, **10**, 429.
10 L. V. Beloussov, N. N. Louchinskaia and A. A. Stein, *Dev. Genes Evol.*, 2000, **210**, 92.
11 R. Gordon, *Int. J. Dev. Biol.*, 2006, **50**, 245.
12 L. V. Beloussov, *Phys. Biol.*, 2008, **5**, 015009.
13 J. J. Tomasek, G. Gabbiani, B. Hinz, C. Chaponnier and R. A. Brown, *Nat. Rev. Mol. Cell Biol.*, 2002, **3**, 349.
14 F. Grinnell, *J. Cell Biol.*, 1994, **124**, 401.
15 E. A. Zamir, A. Czirok, C. Cui, C. D. Little and B. J. Rongish, *Proc. Natl. Acad. Sci. U. S. A.*, 2006, **103**, 19806.
16 C. Verdier, *J. Theor. Med.*, 2003, **5**, 67.
17 P. A. Pullarkat, P. A. Fernandez and A. Ott, *Phys. Rep.*, 2007, **449**, 29.
18 J. Lee, M. Leonard, T. Oliver, A. Ishihara and K. Jacobson, *J. Cell Biol.*, 1994, **127**, 1957.
19 R. J. Pelham, Jr and L. Wang, *Mol. Biol. Cell*, 1999, **10**, 935.
20 W.-H. Guo, M. T. Frey, N. A. Burnham and Y. L. Wang, *Biophys. J.*, 2008, **90**, 2213.
21 U. S. Schwarz, *Soft Matter*, 2007, **3**, 263.
22 A. Saez, A. Bugin, P. Silberzan and B. Ladoux, *Biophys. J.*, 2005, **89**, L52.
23 J. Solon, I. Levental, K. Sengupta, P. C. Georges and P. A. Janmey, *Biophys. J.*, 2007, **93**, 4453.
24 D. Choquet, D. P. Felsenfeld and M. P. Sheetz, *Cell*, 1997, **88**, 39.
25 D. Riveline, E. Zamir, N. Q. Balaban, U. S. Schwarz, T. Ishizaki, S. Narumiya, Z. Kam, B. Geiger and A. D. Bershadsky, *J. Cell Biol.*, 2001, **153**, 1175.
26 A. Zemel and S. A. Safran, *Phys. Rev. E: Stat., Nonlinear, Soft Matter Phys.*, 2007, **76**, 021905.
27 V. S. Deshpande, R. M. McMeeking and A. G. Evans, *Proc. Natl. Acad. Sci. U. S. A.*, 2006, **103**, 14015.
28 U. S. Schwarz and S. A. Safran, *Phys. Rev. Lett.*, 2002, **88**, 048102.
29 I. B. Bischofs and U. S. Schwarz, *Proc. Natl. Acad. Sci. U. S. A.*, 2003, **100**, 9274.
30 C. A. Reinhart-King, M. Dembo and D. A. Hammer, *Biophys. J.*, 2008, **95**, 6044.
31 V. Vogel and M. Sheetz, *Nat. Rev. Mol. Cell Biol.*, 2006, **7**, 265.
32 J. A. Pedersen and M. A. Swartz, *Ann. Biomed. Eng.*, 2005, **33**, 1469.
33 F. Pampaloni, E. G. Reynaud and E. H. K. Stelzer, *Nat. Rev. Mol. Cell Biol.*, 2007, **8**, 839.
34 A. R. Bausch and K. Kroy, *Nat. Phys.*, 2006, **2**, 231.
35 Y. C. Fung, *Biomechanics: Mechanical Properties of Living Tissues*, Springer Verlag, New York, 1993.
36 P. Fernandez, P. A. Pullarkat and A. Ott, *Biophys. J.*, 2006, **90**, 3796.
37 P. Fernandez and A. Ott, *Phys. Rev. Lett.*, 2008, **100**, 238102.
38 P. A. Janmey, M. E. Cormick, S. Rammensee, J. L. Leight, P. C. Georges and F. C. MacKintosh, *Nat. Mater.*, 2007, **6**, 48.
39 P. L. Chandran and V. H. Barocas, *J. Biomech. Eng.*, 2004, **126**, 152.
40 E. Tamariz and F. Grinnell, *Mol. Biol. Cell*, 2002, **13**, 3915.
41 C. Guidry and F. Grinnell, *Coll. Rel. Res.*, 1986, **6**, 515.
42 K. Takakuda and H. Miyairi, *Biomaterials*, 1996, **17**, 1393.
43 A. F. Straight, A. Cheung, J. Limouze, I. Chen, N. J. Westwood, J. R. Sellers and T. J. Mitchison, *Science*, 2003, **299**, 1743.
44 M. Eastwood, V. C. Mudera, D. A. McGrouther and R. A. Brown, *Cell Motil. Cytoskeleton*, 1998, **40**, 13.
45 K. Schmoller, O. Lieleg and A. R. Bausch, *Soft Matter*, 2008, **4**, 2365.
46 I. B. Bischofs and U. S. Schwarz, *Acta Biomater.*, 2006, **2**, 253.
47 R. De, A. Zemel and S. A. Safran, *Nat. Phys.*, 2007, **3**, 655.
48 I. B. Bischofs, F. Klein, M. Lehnert, D. Bastmeyer and U. S. Schwarz, *Biophys. J.*, 2008, **95**, 3488.
49 C. M. Nelson, R. P. Jean, J. L. Tan, W. F. Liu, N. J. Sniadecki, A. A. Spector and C. S. Chen, *Proc. Natl. Acad. Sci. U. S. A.*, 2005, **102**, 11594.
50 H. Kodama, Y. Amagai, H. Sudo, S. Kasai and S. Yamamoto, *Jpn. J. Oral Biol.*, 1981, **23**, 899.
51 G. J. Todaro and H. Green, *J. Cell Biol.*, 1963, **17**, 299.
52 G. J. Todaro, K. Habel and H. Green, *Virology*, 1965, **27**, 179.
53 H. G. Drexler, W. Dirks, W. R. A. F. MacLeod, H. Quentmeier, K. G. Steube and C. C. Uphoff, *DSMZ Catalogue of Human and Animal Cell Lines*, Braunschweig, 2001.
54 M. F. Beatty, *Appl. Mech. Rev.*, 1987, **40**, 1699.
55 F. Grinnell and C. R. Lamke, *J. Cell Sci.*, 1984, **66**, 51.